Cureus Journal of Engineering
https://doi.org/10.7759/s44388-025-00088-x

Original Article

Evaluation of Young's Modulus for Al-Al_2O_3 Functionally Graded Clamped-Free Beams Fabricated by Powder Metallurgy Process

Pravin Malik [1], Ravikiran Kadoli [1]

1. *Department of Mechanical Engineering, National Institute of Technology Karnataka, Surathkal, Mangalore, IND*

Received: May 10, 2026 | Review began: May 11, 2026 | Review ended: August 31, 2026 | Published: November 24, 2026

© **Copyright** 2026
This is an open access article distributed under the terms of the Creative Commons Attribution License CC-BY 4.0., which permits unrestricted use, distribution, and reproduction in any medium, provided the original author and source are credited.

Abstract

This study explores the static deflection and free vibration characteristics of functionally graded aluminum-alumina (Al-Al_2O_3) beams fabricated using the powder metallurgy technique. The beams are constructed in three configurations comprising 5, 6, and 7 layers with ceramic volume fractions of 10%, 20%, and 50% in the outermost layer. Experimental investigations yield data on static deflections, surface strains, and natural frequencies under clamped-free boundary conditions. The bulk Young's modulus of the layered beams is derived from the measured deflection and strain data, showing a deviation of 19%. This modulus is subsequently used to estimate the natural frequency through a lumped mass model, resulting in a close match with experimental observations within a 9% discrepancy. These results underscore the importance of incorporating graded material properties in the accurate modeling and analysis of functionally graded beams.

Categories: Advanced Manufacturing Technologies, Advanced Materials, Materials Engineering

Keywords: powder metallurgy process, functionally graded material, rule of mixture, static deflection, strain, young's modulus

Introduction

Functionally graded structures are engineered materials in which the volume fractions of two or more constituents vary gradually along one or more spatial dimensions. A common example of a functionally graded material (FGM) used in high-temperature applications is a composite of ceramic and metal. Unlike conventional composites, FGMs exhibit smooth transitions in material properties, which helps minimize mechanical and thermal stress concentrations. This makes them well-suited for various engineering applications and a promising alternative to traditional laminated composites. However, the manufacturing of FGMs poses significant challenges, particularly in producing defect-free components. Various fabrication techniques have been explored, as reviewed by Kieback et al. [1], Sobczak and Drenchev [2], and Naebe and Shirvanimoghaddam [3]. These reviews also highlight the importance of understanding the microstructural characteristics of FGMs and emphasize the need for modeling the manufacturing processes to optimize parameters, reduce production costs, and minimize defects. Saleh et al. [4] provided a comprehensive overview of the design and fabrication strategies for smoothly graded FGMs, summarizing the key challenges and benefits based on three decades of research. In addition, Boggarapu et al. [5] investigated the mechanical and tribological behavior of a five-layered Al/Cu FGM produced via powder metallurgy. Bhattacharyya et al. [6] examined the microstructure, micro-hardness, porosity, and flexural strength of functionally graded beams made from Al-SiC and Ni-Al_2O_3 systems, where the ceramic content varied from 10% to 40%.

How to cite this article:
Malik P, Kadoli R (November 24, 2026) Evaluation of Young's Modulus for Al-Al_2O_3 Functionally Graded Clamped-Free Beams Fabricated by Powder Metallurgy Process. Cureus J Eng 3 : es44388-025-00088-x. DOI https://doi.org/10.7759/s44388-025-00088-x

In the study of FGMs, particularly in relation to static deflection and vibration behavior, it is essential not only to prepare appropriate test specimens but also to accurately determine their physical properties. This is especially critical for FGMs fabricated through powder compaction methods, where porosity plays a significant role in influencing material properties. Matuła et al. [7] introduced an innovative powder metallurgy technique to produce two-zoned graded materials with controlled porosity. Phani and Niyogi [8] developed a semi-empirical relationship to estimate the properties of alumina based on porosity, comparing their model with several existing porosity-elastic modulus formulations. Similarly, Asmani et al. [9] utilized wave velocity data to study the effects of porosity, pore size, and distribution on the elastic modulus of alumina pellets. Kováčik [10] applied percolation theory to model the dependence of Young's modulus on porosity. Chawla and Deng [11] explored the impact of porosity on several mechanical properties including Young's modulus, tensile strength, microstructure, strain-to-failure, and fatigue strength for Fe-0.85Mo-Ni steels produced via powder metallurgy. Savchenko et al. [12] conducted compression tests on alumina cylindrical specimens with varying porosity, examining its effects on shear strength, shear modulus, and modulus of elasticity. Wattanasakulpong and Ungbhakorn [13] incorporated porosity into the rule of mixtures, allowing for effective material property predictions that account for porosity. Their findings highlighted how porosity levels influence the frequency response of functionally graded beams. Further research on the free vibration behavior of functionally graded (FG) beams produced by different techniques such as hot isostatic pressing, sequential infiltration, and plasma spraying has been conducted by Kapuria et al. [14], Wattanasakulpong et al. [15], and Malik and Kadoli [16], respectively.

To the best of the author's knowledge, there are no existing experimental studies that investigate the static deflection, strain, and natural frequencies of Al-Al_2O_3 FG beams fabricated via powder metallurgy under clamped-free boundary conditions. In this study, analytical methods are used to estimate the natural frequencies, which are then validated against experimental results. The Young's modulus of the FG beams is determined through deflection and strain measurements. This experimentally derived bulk modulus is subsequently used to compute the numerical natural frequencies using a lumped mass model.

Materials And Methods

Material gradation through the thickness of functionally graded beam

Consider an FG beam with rectangular cross section. Let l,b, and h be the length, width, and thickness of the beam. The *x*-coordinate is considered at the mid-plane along the length of the beam and *y*-coordinate is taken along the width of the beam. Figure *1* represents FG beam with stepwise material gradation. The material property of each layer is considered as per the rule of mixture along the *z* direction. Each layer having a mixture of ceramic and metal with volume fractions V_c and V_m, and simple rule of mixture holds true.

$$V_c + V_m = 1 \tag{1}$$

The effective material property, for each layer of the step-wise graded FG beam is given by the relation

$$P_{\text{eff}}(z) = P_m V_m(z) + P_c V_c(z) \tag{2}$$

where, P and V represents a physical property and volume fraction, which varies along the thickness direction *z* coordinate. Subscript c and m indicate ceramic and metal, respectively.

How to cite this article:
Malik P, Kadoli R (November 24, 2026) Evaluation of Young's Modulus for Al-Al_2O_3 Functionally Graded Clamped-Free Beams Fabricated by Powder Metallurgy Process. Cureus J Eng 3 : es44388-025-00088-x. DOI https://doi.org/10.7759/s44388-025-00088-x

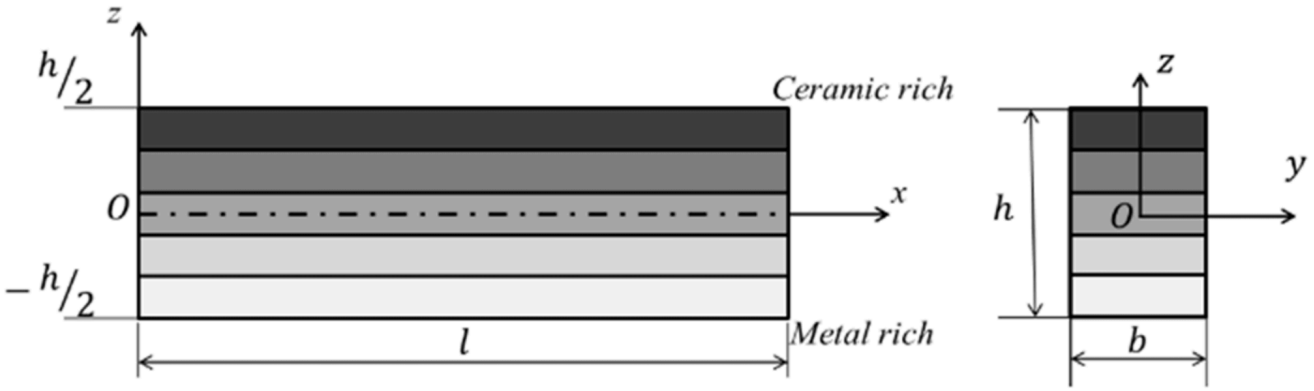

FIGURE 1: FG beam with step-wise gradation along its thickness

FG, functionally graded

Semi-empirical approach to calculate the Young's Modulus

This study aims to determine the Young's modulus of the material without damaging the beam samples in tensile testing. The Young's modulus is calculated using two different methods: the deflection equation and the flexure equation. Experimental deflection data for the beam under various loads are applied to the deflection equation derived from beam theory. Strains on the beam's surface are measured by attaching a strain gauge, and these measurements are then used in the flexural relation to calculate the Young's modulus.

For a clamped-free beam with load applied at the free end, the deflection at any point along the length is given by Gere [17],

$$w(x) = \frac{P}{6EI}\left(3lx^2 - x^3\right) \tag{3}$$

Equation (3) can be re-written as

$$E = \frac{P}{6w(x)I}\left(3lx^2 - x^3\right) \tag{4}$$

where E is modulus of elasticity, $w(x)$ is the deflection of the beam at a distance x form the fixed end, P is the transverse point load applied at free end, l is the effective length (i.e. from the fixed end to free end of the beam) of the beam, I is the moment of inertia of the beam.

The flexural equation for a beam is provided as follows [17]:

$$\frac{M}{I} = \frac{\sigma_b}{y} = \frac{E}{R} \tag{5}$$

The bending moment, M and bending stress, σ_b at the support are defined as

$$M = Pl \tag{6}$$

$$\sigma_b = \varepsilon_b E \tag{7}$$

where P, l, ε_b, and E are the applied load, effective length, bending strain developed due to load application, and modulus of elasticity of the beam, respectively. Assuming that the neutral axis and the central axis of the beam coincide, $y = h/2$, where, h is thickness of the FG beam. By substituting all the terms in Equation (5), the modulus of elasticity of beam can be written as

$$E = \frac{Plh}{2\varepsilon_b I} \tag{8}$$

$\in_b$ is the experimentally obtained strain from the strain gauge bonded on the top surface of the FG beam.

Analytical free vibration natural frequency of beam

Two approaches are available for analytically calculating the natural frequency of beams: the lumped mass system and the continuous system. In lumped mass system, the beam is assumed mass-less and the entire beam mass is assumed to be replaced by a concentrated mass at the free end. The natural frequency of the beam based on lumped mass system is given as

$$\omega_n = \sqrt{\frac{3EI}{m_c l^3}} \tag{9}$$

where, E is the bulk Young's modulus of the beam material (calculated from deflection and bending equations), I is the moment of inertia of the beam cross-section, l is the effective beam length, and m_c is an equivalent concentrated mass placed at the free end of the cantilever beam,

$$m_c = \frac{33}{140} m_b \tag{10}$$

where, m_b is mass of beam for effective length l.

Fabrication of functionally graded beams using powder metallurgy process

Three types of FG beams, each having layers of Al-Al_2O_3 of different volume fraction composition along its thickness, fabricated by powder metallurgy process are listed in Table *1*. These fabricated beams are used for experimental studies. Volume fraction of alumina in each layer is varied step wise. Schematic representation of stepped variation of volume fraction of alumina, V_c, versus non-dimensional thickness, $\frac{z}{h}$, in each layer for a FG beam consisting of 5, 6, and 7 layers along its thickness are shown in Figure *2*(a), (b), and (c), respectively.

FG sample type	No. of layers	Percentage composition of Al-Al_2O_3 in each layer of FG beam						
		1	2	3	4	5	6	7
Type 1	5	100:0	98.75:1.25	97.5:2.5	95:5	90:10	-	-
Type 2	6	100:0	98.75:1.25	97.5:2.5	95:5	90:10	80:20	-
Type 3	7	100:0	98.75:1.25	97.5:2.5	95:5	90:10	80:20	50:50

TABLE 1: Percentage composition of Al-Al2O3 in each layer for three different types of FG beams

FG, functionally graded

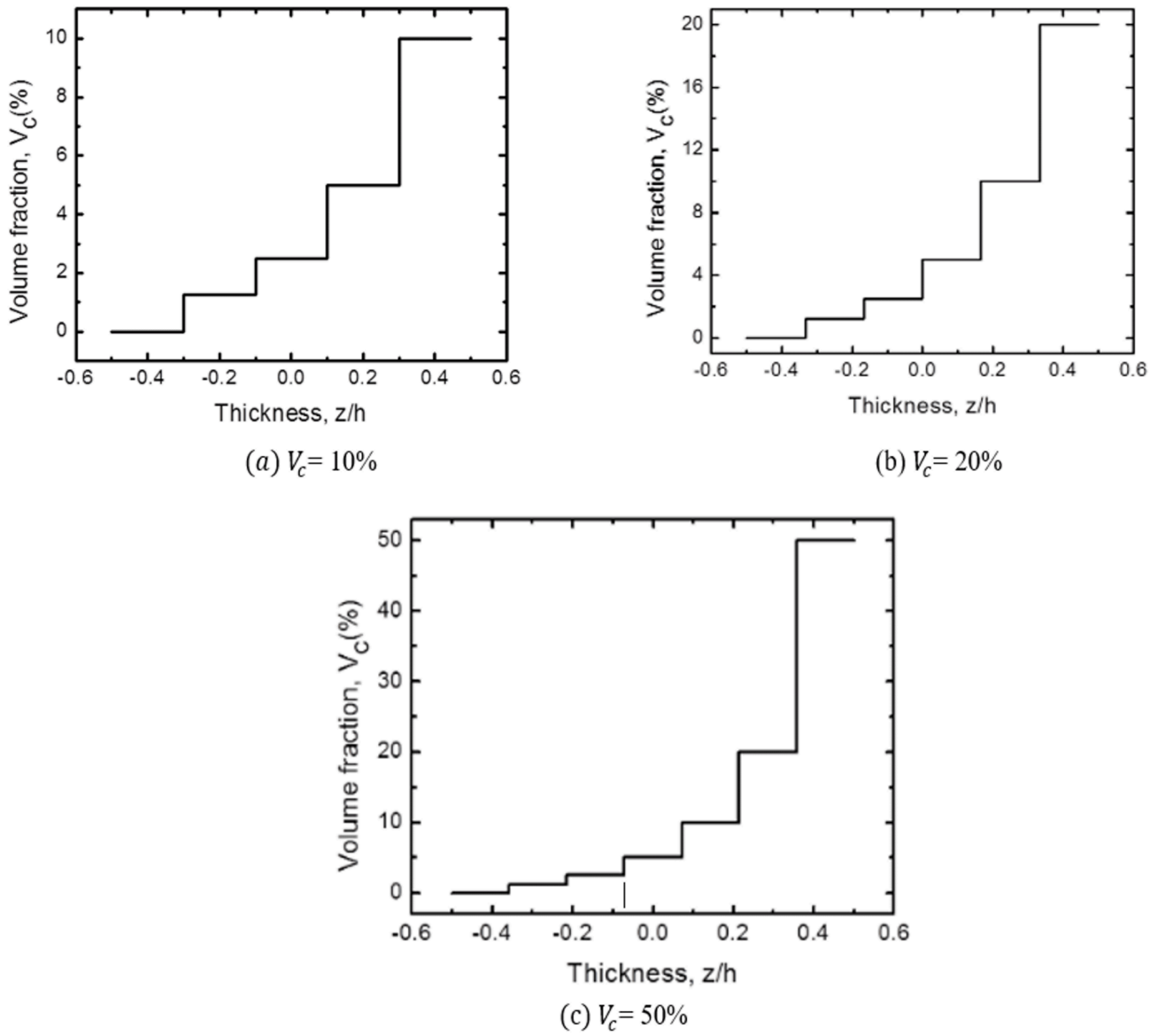

FIGURE 2: Variation of volume fraction with respect to thickness of FG beam; (a) volume fraction 10%, (b) volume fraction 20%, and (c) volume fraction 50%

FG, functionally graded

The thickness of each layer in the five-layer (Type-1) beam was approximately between 0.45 mm and 0.5 mm depending on the weight of the powder used for each layer. The ceramic content in the layers of the beam samples were from 0% to 10% with the bottom layer being of pure metal and the top layer having 10% ceramic content. The five-layered FG beam sample had Al_2O_3 composition as 0/1.25/2.5/5/10% from bottom to top layer. The metal and ceramic constituents were mixed thoroughly in a planetary ball mill and laid layer by layer in a die. The powder laid in the die was compacted using universal testing machine. After compaction the samples were subjected to sintering. The sintering temperature was varied linearly until the final sintering temperature of 660°C was attained. The length of the sample used in present study was 150 mm and had a cross section of approximately 21 × 2.5 mm for FGM - Type 1. Similarly, FG beams of 6 and 7 layers were produced wherein the ceramic volume fraction was 20% and 50% on the ceramic rich outer most layer as shown in Figure *2*(b) and (c) respectively. The thickness of each layer was again maintained between 0.4 mm and 0.5 mm. The thickness depends on the weight of the powder. The average weight of the powder for pure aluminium layer is 3.4 g and

for different FG layers it varies from 3.442 g to 4.8 g. The details of the properties of the material considered for calculations are in Table 2. A high precision weigh balance (CONTECH electronic balance CAI-234) was used to measure the mass of the powder. Considering all these parameters, it is found that the beam thickness after fabrication is between 2.2 mm and 3.25 mm. Following are the parameters used for preparing the Al-Al_2O_3 FGM beam samples using powder metallurgy process:

- Die wall lubricant: Zinc stearate.
- Binding agent: Ethanol.
- Load applied: 60 tons.
- Loading duration: 5 min.
- Green compacting load: 10 tons for 1 min.
- Sintering temperature: 660°C.
- Stepwise increase of temperature: 10°C per min.
- Sintering duration: 5 hours.
- Cooling: Furnace cooling.

Material	Young's modulus, E (GPa)	Density, ρ (kg/m^3)	Poisson's ratio, ν
Aluminium	69.0	2,698	0.26
Alumina (Al_2O_3)	349.55	3,750	0.33

TABLE 2: Material properties of Aluminium and Al2O3

S. no.	FG sample	Number of layers	Volume fraction of Al_2O_3 in each layer	Mass of beam (grams)	Length (mm)	Average width (mm)	Average thickness (mm)
1	FGM-19	5	0,1.25,2.5,5,10	17.743	151.82	20.722	2.476
2	FGM-20	5	0,1.25,2.5,5,10	17.737	151.46	20.716	2.49
3	FGM-23	5	0,1.25,2.5,5,10	17.572	152.44	21.484	2.224
4	FGM-24	5	0,1.25,2.5,5,10	17.182	152.3	21.472	2.344
5	FGM-25	5	0,1.25,2.5,5,10	16.867	152.3	21.468	2.22
6	FGM-26	6	0,1.25,2.5,5,10 ,20	20.149	152.73	21.674	2.716

7	FGM-27	6	0,1.25,2.5,5,10,20	20.504	152.54	21.582	2.622
8	FGM-28	6	0,1.25,2.5,5,10,20	20.155	152.3	21.606	2.582
9	FGM-29	5	0,1.25,2.5,5,10	18.498	152.71	21.676	2.358
10	FGM-30	6	0,1.25,2.5,5,10,20	20.926	152.56	21.65	2.684
11	FGM-31	7	0,1.25,2.5,5,10,20,50	24.716	152.87	21.664	3.254
12	FGM-32	7	0,1.25,2.5,5,10,20,50	24.156	153.62	21.782	3.14
13	FGM-33	6	0,1.25,2.5,5,10,20	20.657	153.43	21.682	2.666
14	FGM-34	7	0,1.25,2.5,5,10,20,50	24.211	153.56	21.738	3.21
15	FGM-35	7	0,1.25,2.5,5,10,20,50	24.573	153.24	21.8	3.208
16	FGM-36	6	0,1.25,2.5,5,10,20	20.821	152.55	21.466	2.62
17	FGM-37	7	0,1.25,2.5,5,10,20,50	24.643	153.5	21.584	3.25
18	FGM-38	5	0,1.25,2.5,5,10	17.344	153.04	21.634	2.17
19	FGM-39	5	0,1.25,2.5,5,10	17.477	153.72	21.642	2.234
20	FGM-40	5	0,1.25,2.5,5,10	17.432	152.72	21.576	2.17
21	FGM-41	6	0,1.25,2.5,5,10,20	20.831	152.74	21.652	2.62

TABLE 3: Details of volume fraction composition, mass, and dimensions of beams fabricated by powder metallurgy process

The above-mentioned parameters were maintained the same while fabricating the FG beam samples for study. A total of 21 samples of 3 different FG compositions were prepared. The specifications, like beam composition, beam weight, beam length, width, and thickness, are listed in Table *3*. The width and thickness of the beams are measured at five locations along the beam length and the average of these measurements was considered.

Experimental setup for static deflection analysis of FG beams

The schematic diagram depicting the measurement of static deflection of the clamped-free beam is shown in Figure *3*. The sample was loaded with a concentrated load at the free end. Standard weights of 50 g, 70 g, 100 g, 130 g, and 150 g are used to apply the load. The beam's deflection was recorded using a laser optical displacement sensor with a resolution of 1 micron and a sampling rate of 10 ms. The sensor's analog output is transmitted to a computer via an RS422 analog-to-digital USB converter. The readings are collected on the computer using ILD1402 software. The deflection readings are taken at the free end, with the difference between the readings before and after the load is applied being recorded as the beam displacement.

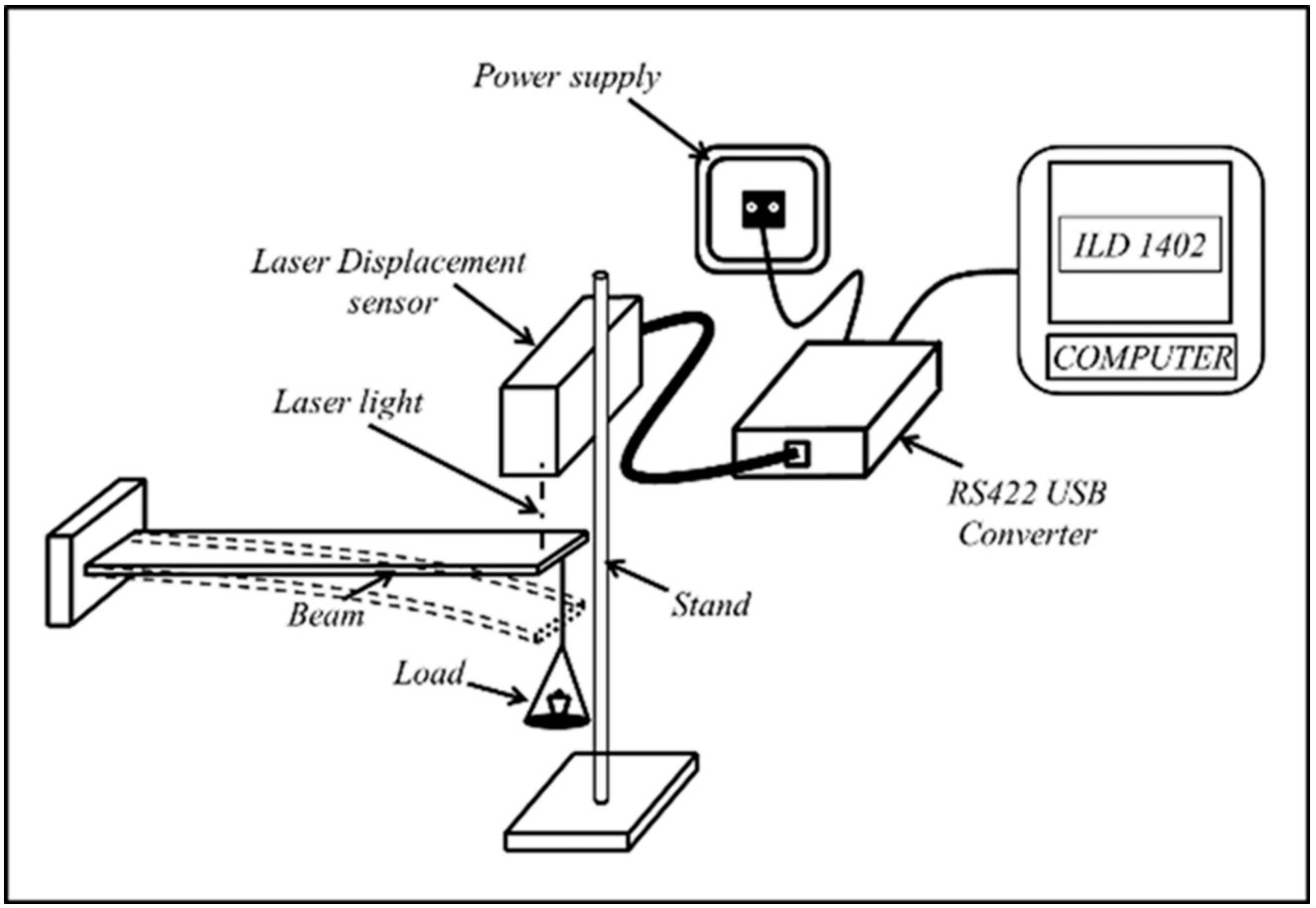

FIGURE 3: Schematic representation of experimental setup to measure the deflection of clamp-free beam

Experimental setup to measure the surface strain using strain gauge

The surface of the beam is first cleaned with acetone to remove any dust particles. A metallic strain gauge with a nominal resistance of 350 ohms, a gauge factor (GF) of 2, and a 5 mm gauge length is mounted along the beam, approximately 20 mm from the fixed end, using epoxy adhesive. Strain measurements are taken for the FG beams under a clamp-free boundary condition. Various accessories used for experimental strain measurement are shown in Figure *4*. The strain gauge is connected in a quarter-bridge configuration. The beam is subjected to a point load at its free end, causing deflection. Strain data are directly acquired using the LABVIEW 2012 software in conjunction with the NI9237 data acquisition system. The number of samples and the sampling rate are set to 2,500 and 2,500 Hz, respectively. Strains corresponding to different loadings are recorded for further calculations.

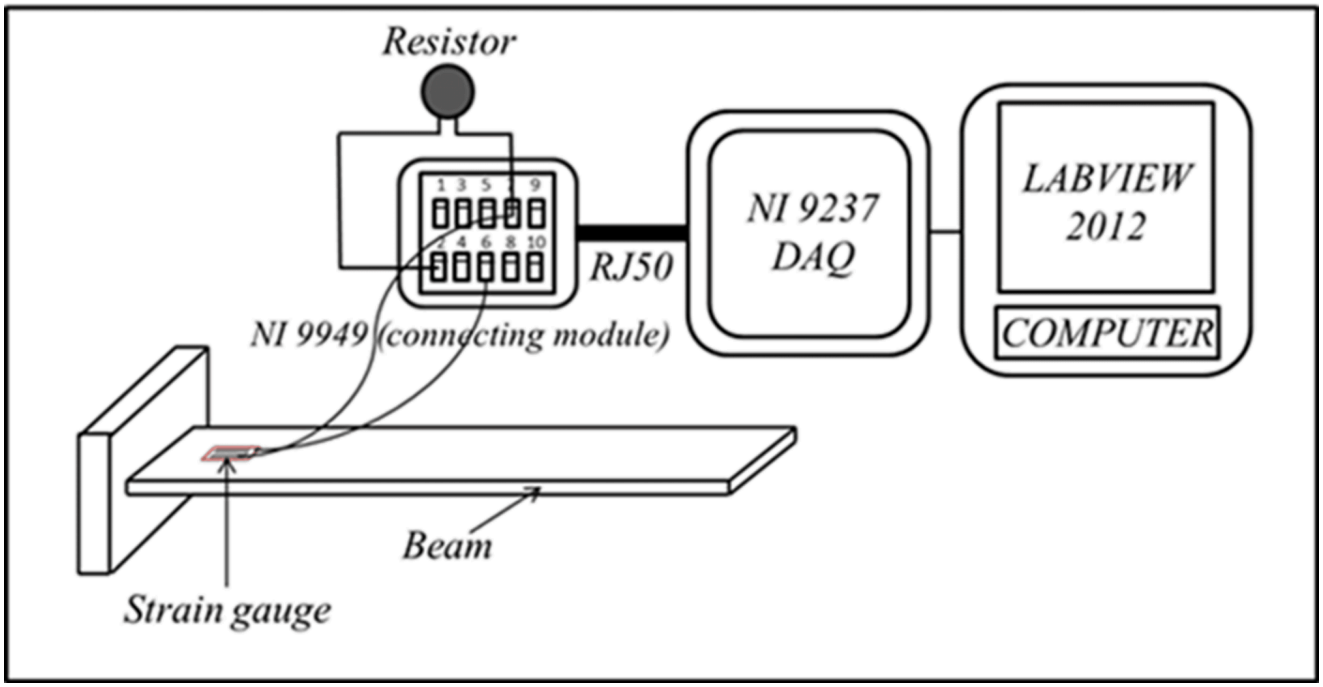

FIGURE 4: Block diagram of experimental setup to measure the surface strain using strain gauge

Experimental set-up for free vibration natural frequency analysis of FG beams

The free vibration natural frequency of FG beams is determined using the impact hammer testing method. An impulse is applied to the clamped-free beam, as shown in Figure *5*. The resulting response is recorded using a laser displacement sensor. The displacement signals from the laser sensor are collected on a computer using ILD1402 software. The fast Fourier transform of the time domain response was computed using data processing software to obtain the frequency response. The peak locations give the natural frequencies at various modes.

How to cite this article:
Malik P, Kadoli R (November 24, 2026) Evaluation of Young's Modulus for Al-Al_2O_3 Functionally Graded Clamped-Free Beams Fabricated by Powder Metallurgy Process. Cureus J Eng 3 : es44388-025-00088-x. DOI https://doi.org/10.7759/s44388-025-00088-x

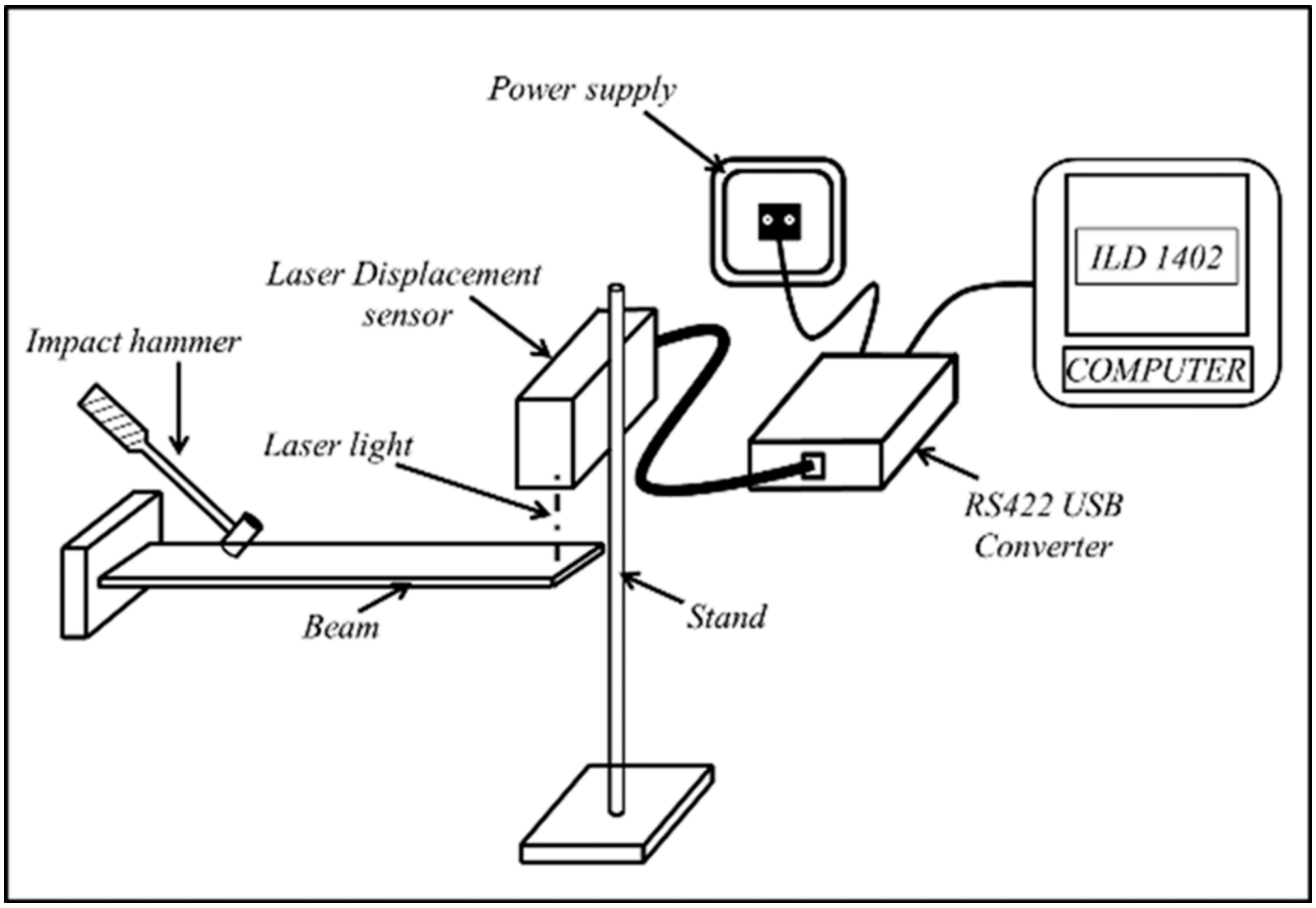

FIGURE 5: Schematic representation of experimental setup to measure the free vibration natural frequency of beams

Results And Discussion

Young's Modulus of elasticity from deflection equation and flexural equation

For all the FG beams, deflection was measured for the applied loads corresponding to masses of 50 g, 70 g, 100 g, 130 g, and 150 g, as shown in Table *4*. Using the deflection values for the applied loads in Equation (4), the Young's modulus is calculated. For the range of applied loads and the resulting deflections, the Young's modulus is computed for each FG beam, and the average value is taken for further calculations. The same procedure is followed for the strain data: for loads of 50 g, 70 g, 100 g, 130 g, and 150 g, the corresponding surface strains are recorded. These strain values for the different loads are presented in Table *5*.

S. no.	FG beam sample	FGM type	Deflection at the free end for various loads, mm				
			50 g	70 g	100 g	130 g	150 g
1	FG-19	Type-1	0.634	0.906	1.297	1.702	1.967
2	FG-20	Type-1	0.464	0.666	0.975	1.289	1.495
3	FG-23	Type-1	0.423	0.595	0.842	1.118	1.303

4	FG-25	Type-1	0.435	0.605	0.862	1.126	1.305
5	FG-29	Type-1	0.446	0.619	0.901	1.178	1.370
6	FG-38	Type-1	0.487	0.677	0.979	1.283	1.462
7	FG-39	Type-1	0.552	0.775	1.126	1.477	1.712
8	FG-40	Type-1	0.537	0.748	1.085	1.407	1.668
9	FG-30	Type-2	0.386	0.533	0.775	1.033	1.194
10	FG-41	Type-2	0.421	0.593	0.868	1.130	1.313
11	FG-31	Type-3	0.282	0.389	0.568	0.748	0.871
12	FG-35	Type-3	0.295	0.413	0.584	0.774	0.891

TABLE 4: Deflection data of FG beams at various loads

FG, functionally graded

S. no.	FG beam sample	FGM type	Strain measured for various loads, 10^{-6} ppm				
			50 g	70 g	100 g	130 g	150 g
1	FG-19	Type-1	124.55	176.813	252.607	334.394	387.439
2	FG-20	Type-1	94.298	131.170	190.854	250.266	288.393
3	FG-23	Type-1	84.637	115.625	166.177	219.009	251.797
4	FG-25	Type-1	76.880	106.945	154.343	202.065	234.224
5	FG-29	Type-1	90.534	134.089	188.968	248.038	286.711
6	FG-38	Type-1	85.346	119.435	172.615	225.586	260.249
7	FG-39	Type-1	96.078	135.797	197.104	257.675	301.409
8	FG-40	Type-1	88.839	129.220	188.496	245.858	287.657
9	FG-30	Type-2	75.221	106.627	155.812	202.939	238.820
10	FG-41	Type-2	81.800	126.701	179.319	222.419	258.478
11	FG-31	Type-3	93.134	125.701	181.807	244.314	286.273

How to cite this article:
Malik P, Kadoli R (November 24, 2026) Evaluation of Young's Modulus for Al-Al_2O_3 Functionally Graded Clamped-Free Beams Fabricated by Powder Metallurgy Process. Cureus J Eng 3 : es44388-025-00088-x. DOI https://doi.org/10.7759/s44388-025-00088-x

12	FG-35	Type-3	85.328	117.061	167.271	222.617	260.58

TABLE 5: Strain data of FG beams at various loads

FG, functionally graded; FGM, functionally graded material

Using Equation (8), the Young's modulus is calculated for each load-strain pair, and the average Young's modulus is then used for subsequent calculations. The Young's modulus of FG beams, calculated using the deflection and flexural equations, is presented in Table *6*. It is important to note that the values obtained from the deflection data and the strain data do not align, with a deviation of approximately 19%. Several factors may contribute to this variation, including: (i) the FG beam samples, fabricated using the powder metallurgy process, have a poorly densified structure, and (ii) there may be the presence of porosity in the fabricated samples [9]. Also, the residual stresses arising from differences in thermal expansion coefficients between Al and Al_2O_3 can influence stiffness and deflection behavior, and while not quantified in the present study, they should be considered when interpreting the mechanical performance of Al-Al_2O_3 FGMs.

S. no.	FG beam sample	FGM type	Modulus of elasticity (GPa)		Error %
			Deflection equation	Flexural equation	
1	FG-19	Type-1	19.93	23.72	16.0
2	FG-20	Type-1	26.24	31.30	16.2
3	FG-23	Type-1	40.30	43.02	6.3
4	FG-25	Type-1	39.81	46.81	15.0
5	FG-29	Type-1	31.78	33.65	5.6
6	FG-38	Type-1	37.64	43.62	13.7
7	FG-39	Type-1	29.99	36.06	16.8
8	FG-40	Type-1	33.98	40.44	16.0
9	FG-30	Type-2	24.89	30.80	19.2
10	FG-41	Type-2	24.26	29.71	18.3
11	FG-31	Type-3	14.23	16.34	12.9
12	FG-35	Type-3	19.11	20.06	4.7

TABLE 6: Young's modulus evaluated from deflection and flexural equation

FG, functionally graded; FGM, functionally graded material

Statistically, from Table 6, the Type-1 beams (n = 8) exhibited a mean modulus of 32.92 GPa with a relatively high standard deviation (7.36 GPa), reflecting moderate reproducibility and wider variability compared to other beam types. The flexural equation consistently overestimated values relative to deflection, with a mean error of 14.9%, highlighting systematic bias. Importantly, the clamped-free condition may not represent a perfectly fixed support, and fixture flexibility or load application uncertainties could have influenced deflection measurements. For Type-2 and Type-3 beams, only two samples each were available, limiting statistical strength. Type-2 beams showed excellent reproducibility (mean modulus 24.58 GPa, SD 0.45 GPa) but the highest systematic error (18.8%), while Type-3 beams had moderate reproducibility (mean modulus 16.67 GPa, SD 3.45 GPa) and smaller error (8.8%). Overall, reproducibility and accuracy varied strongly with beam type: Type-1 beams were the least consistent, Type-2 beams the most reproducible but biased, and Type-3 beams offered balanced though limited insights. These findings emphasize the need to account for fixture compliance and load uncertainties in future work to strengthen confidence in modulus measurements.

Free vibration frequency of FG beams

The modulus of elasticity of the FG beams, calculated using experimental deflection and strain readings, is used to determine the natural frequency analytically. This calculated natural frequency is then compared with the experimentally measured frequencies obtained using the strain gauge and laser displacement sensor. In Table 7, the natural frequency, calculated by considering a lumped mass system using the Young's modulus obtained from both deflection and strain data, is presented. It is observed that the analytical natural frequency results from both methods are close to the experimental values. However, it is important to note that the natural frequency values derived using the Young's modulus from the bending equation and the flexural equation do not align. The natural frequency calculated using the Young's modulus from the flexural equation is higher compared to that obtained from the deflection equation.

S. no.	FG beam sample	FGM type	Experimental frequency (laser sensor) Hz	Experimental frequency (strain gauge) Hz	Analytical frequency (deflection equation) Hz	Analytical frequency (flexure equation) Hz	Error % (laser sensor/deflection equation)	Error % (strain gage/flexure equation)
1	FGM-19	Type-1	77.96	71.0	71.52	77.48	-9.00	8.36
2	FGM-20	Type-1	85.70	85.0	82.08	89.66	-4.41	5.20
3	FGM-23	Type-1	88.74	89.0	88.14	91.07	-0.68	2.27
4	FGM-25	Type-1	94.27	96.0	89.11	96.62	-5.79	0.64
5	FGM-29	Type-1	81.32	81.0	83.74	86.17	2.89	6.00
6	FGM-38	Type-1	85.97	86.0	83.09	89.45	-3.47	3.86
7	FGM-39	Type-1	79.88	79.0	77.36	84.83	-3.26	6.87
8	FGM-40	Type-1	79.42	80.0	78.57	85.70	-1.08	6.65
9	FGM-30	Type-2	89.89	88.0	84.52	94.03	-6.35	6.41
10	FGM-41	Type-2	83.05	83.0	80.71	89.31	-2.90	7.07
11	FGM-31	Type-3	95.63	92.9	95.39	102.25	-0.25	9.14

How to cite this article:
Malik P, Kadoli R (November 24, 2026) Evaluation of Young's Modulus for Al-Al_2O_3 Functionally Graded Clamped-Free Beams Fabricated by Powder Metallurgy Process. Cureus J Eng 3 : es44388-025-00088-x. DOI https://doi.org/10.7759/s44388-025-00088-x

12	FGM-35	Type-3	93.16	89.6	89.81	90.20	-3.73	-0.33

TABLE 7: Analytical natural frequency of clamped-free beams using Young's modulus calculated from deflection equation and flexure equation and its comparison with the experimental natural frequency

FG, functionally graded; FGM, functionally graded material

Conclusions

In a FG beam, the material constituents are graded across the thickness. The physical properties change from layer to layer primarily due to the fact that the volume fractions of metal or ceramic are not the same. Theoretically, it is possible to use the rule of mixture for calculation of effective properties. Experimental determination of the contribution of each layer to the overall physical property is difficult to determine. This study provides a comprehensive experimental and theoretical investigation of the static deflection, strain, and free vibration behavior of FG beams. Experimental measurements of beam deflection and surface strain were used to calculate the bulk Young's modulus. The deflections of the beam or the strains measured on the surface of the beam at a point are macroscopic changes. Hence, the Young's modulus evaluated is called the bulk Young's modulus of the FG beam. However, the bulk Young's modulus thus determined deviates considerably, with a 19% difference for various FG beam combinations. The bulk Young's modulus was used as the input data to calculate the free vibration natural frequency of the beams through analytical equations considering a lumped mass system. The experimental results revealed good agreement within 9% between the natural frequency and the numerical predictions using the calculated bulk Youngs modulus using deflection and flexure equation. Apart from this, the natural frequency evaluated using the time domain data obtained using the laser sensor and the strain gauge data were in close agreement. The minor deviations are likely attributed to defects in the FG beam samples, particularly the presence of porosity. This defect is believed to affect key material properties, including density and Young's modulus, which in turn influence the beam's structural behavior.

The findings underscore the need for refinement in the powder metallurgy process, particularly in controlling the sintering temperature, to minimize porosity and improve material consistency. Future work should focus on developing more accurate models that incorporate porosity effects, enabling the prediction of true material properties, such as Young's modulus and density, for FG beams produced through powder metallurgy.

Additional Information

Author Contributions

All authors have reviewed the final version to be published and agreed to be accountable for all aspects of the work.

Concept and design: Pravin Malik, Ravikiran Kadoli

Acquisition, analysis, or interpretation of data: Pravin Malik, Ravikiran Kadoli

Drafting of the manuscript: Pravin Malik, Ravikiran Kadoli

Critical review of the manuscript for important intellectual content: Pravin Malik, Ravikiran Kadoli

Disclosures

Human subjects: All authors have confirmed that this study did not involve human participants or tissue.

Animal subjects: All authors have confirmed that this study did not involve animal subjects or tissue.

Conflicts of interest: In compliance with the ICMJE uniform disclosure form, all authors declare the following:

- **Payment/services info:** All authors have declared that no financial support was received from any organization for the submitted work.
- **Financial relationships:** All authors have declared that they have no financial relationships at present or within the previous three years with any organizations that might have an interest in the submitted work.
- **Other relationships:** All authors have declared that there are no other relationships or activities that could appear to have influenced the submitted work.

Data Availability Statements

The datasets (and/or code) supporting this study are available from the corresponding author upon reasonable request.

References

1. Kieback B, Neubrand A, Riedel H: Processing techniques for functionally graded materials. Materials Science and Engineering: A. 2003, 362:81-106. 10.1016/s0921-5093(03)00578-1
2. Sobczak JJ, Drenchev L: Metallic functionally graded materials: a specific class of advanced composites. Journal of Materials Science & Technology. 2013, 29:297-316. 10.1016/j.jmst.2013.02.006
3. Naebe M, Shirvanimoghaddam K: Functionally graded materials: A review of fabrication and properties. Applied Materials Today. 2016, 5:223-245. 10.1016/j.apmt.2016.10.001
4. Saleh B, Jiang J, Fathi R, et al.: 30 Years of functionally graded materials: An overview of manufacturing methods, applications and future challenges. Composites Part B: Engineering. 2020, 201:108376. 10.1016/j.compositesb.2020.108376
5. Boggarapu V, Rama Sreekanth PS, Peddakondigalla VB: Microstructure, mechanical and tribological properties of Al/Cu functionally graded material fabricated through powder metallurgy. Journal of Engineering Research. 2024, 12:502-510. 10.1016/j.jer.2023.100119
6. Bhattacharyya M, Kumar AN, Kapuria S: Synthesis and characterization of Al/SiC and Ni/Al2O3 functionally graded materials. Materials Science and Engineering: A. 2008, 487:524-535. 10.1016/j.msea.2007.10.040
7. Matuła I, Dercz G, Barylski A, Kubisztal J: Porous functionally graded material based on a new Ti-25Nb-5Zr-(2Sn) alloy produced using the powder metallurgy technique. Journal of Alloys and Compounds. 2024, 982:173779. 10.1016/j.jallcom.2024.173779
8. Phani KK, Niyogi SK: Young's modulus of porous brittle solids. Journal of Materials Science. 1987, 22:257-263. 10.1007/bf01160581
9. Asmani M, Kermel C, Leriche A, Ourak M: Influence of porosity on Young's modulus and Poisson's ratio in alumina ceramics. Journal of the European Ceramic Society. 2001, 21:1081-1086. 10.1016/s0955-2219(00)00314-9
10. Kováčik J: Correlation between Young's modulus and porosity in porous materials. Journal of Materials Science Letters. 1999, 18:1007-1010. 10.1023/a:1006669914946
11. Chawla N, Deng X: Microstructure and mechanical behavior of porous sintered steels. Materials Science and Engineering: A. 2005, 390:98-112. 10.1016/j.msea.2004.08.046
12. Savchenko NL, Sevostyanova IN, Sablina TY, et al.: The influence of porosity on the elasticity and strength of alumina ceramics. Epitoanyag - Journal of Silicate Based and Composite Materials. 2014, 66:44-47. 10.14382/epitoanyag-jsbcm.2014.9
13. Wattanasakulpong N, Ungbhakorn V: Linear and nonlinear vibration analysis of elastically restrained ends FGM beams with porosities. Aerospace Science and Technology. 2014, 32:111-120. 10.1016/j.ast.2013.12.002
14. Kapuria S, Bhattacharyya M, Kumar AN: Bending and free vibration response of layered functionally graded beams: A theoretical model and its experimental validation. Composite Structures. 2008, 82:390-402. 10.1016/j.compstruct.2007.01.019
15. Wattanasakulpong N, Prusty BG, Kelly DW, Hoffman M: Free vibration analysis of layered functionally graded beams with experimental validation. Materials & Design (1980-2015). 2012, 36:182-190. 10.1016/j.matdes.2011.10.049
16. Malik P, Kadoli R: Nonlinear bending and free vibration response of SUS316-Al2O3 functionally graded plasma sprayed beams: theoretical and experimental study. Journal of Vibration and Control. 2016, 24:1171-1184. 10.1177/1077546316659422
17. Gere JM: Mechanics of Materials. Brooks/Cole, Pacific Grove, CA; 2001.